

3D models related to the publication: Shape diversity in conodont elements, a quantitative study using 3D topography.

Alexandre Assemat^{1*}, Ghislain Thiery², Thibaud Lieffroy², Catherine Girard¹

¹ ISEM, Univ Montpellier, CNRS, EPHE, IRD, Montpellier, France.

² PALEVOPRIM, University of Poitiers, UMR CNRS, Poitiers 7262, France.

*Corresponding author: alexandre.assemat@gmail.com

Abstract

The present 3D Dataset contains the 3D models analyzed in Assemat et al. 2023: Shape diversity in conodont elements, a quantitative study using 3D topography. Marine Micropaleontology 184. <https://doi.org/10.1016/j.marmicro.2023.102292>. P1 elements represent dental components of the conodont apparatus that perform the final stage of food processing before ingestion. Consequently, quantifying the shape of P1 elements across the topographic indices of different conodont species becomes crucial for deciphering the diversity in feeding behavior within this group.

Keywords: Conodonts, Doolkit, Morphofunction, Scanning resolution, Topography

Submitted:16/01/2024, published online:17/01/2024. <https://doi.org/10.18563/journal.m3.223>

INTRODUCTION

Conodonts, a successful group of early eel-shaped vertebrates, thrived in seas from the upper Cambrian (-500My) to the end of the Triassic (Clark 1983). Their presence in the fossil record is primarily marked by abundant phosphatic micro-remains known as conodont elements, functioning akin to teeth (Purnell 1995). These elements were intricately organized in a complex feeding apparatus, enabling conodonts to capture and process their prey (Aldridge 1987; Purnell and Donoghue 1997; Goudemand et al. 2011). Among these elements, the pectiniform elements (P1) stand out as the most robust and are typically well-preserved in the fossil record. Operating in pairs, the left and right P1 elements play a crucial role in the final stage of food processing before ingestion. Despite having no living representatives, the functional diversity of conodonts has been explored through nomenclatural descriptions, classification of P1 shapes (e.g., Sweet 1981, 1988; Over 1992; Purnell et al. 2000), morphometry (e.g., Girard et al. 2004; Hogancamp et al. 2016; Guenser et al. 2019), and analysis of platform element articulation kinematics (e.g., Donoghue and Purnell 1999; Martinez-Perez et al. 2014a, b; Suttner et al. 2017). As P1 elements are involved in food bolus processing, their shape may offer insights into diet preferences. While previous studies have investigated P1 element shapes using 2D and 3D morphometrics at the genus or species level, inter-species comparisons face challenges due to the wide morphological disparity and difficulty in finding homologous structures (Purnell et al. 2000; Jones et al. 2009). The advent of 3D imaging has introduced new tools for studying shape variations and diversity, enabling quantitative analyses on a larger scale. Dental topographic analysis, one such tool, divides an occlusal surface into smaller elements, such as points in digital elevation models (Ungar and Williamson 2000; Evans et al. 2007) or small polygons in 3D surfaces (Guy et al. 2013).

Algorithms can then quantify the entire surface morphology using indices of complexity, orientation, or sharpness (Winchester 2016), eliminating the need for homologous structures and allowing a functional perspective on a wide range of morphologies (Evans et al. 2007; Prufrock et al. 2016; Li et al. 2020). While dental topographic methods have primarily been applied to mammal teeth for diet and morphofunctional assessments, applying these indices to conodont elements could facilitate a large-scale quantification of P1 element shape diversity. This approach may provide a better understanding of their morphofunctional role in the food processing of this extinct group, addressing poorly explored aspects such as sharpness, average slope, and complexity. This study aims to test the relevance and limitations of available indices for the quantitative segregation of shapes in several conodont P1 elements, considering the impact of 3D mesh processing on topographical results, including the initial voxel size and triangle homogenization. With that in mind, the topographical indices represent a promising toolkit for the quantification of conodonts shapes diversity as they allow to segregate sharp blade-like morphologies from wider platform ones (see Fig. 1). Its further implication to constrain the functional part of the P elements during food processing could bring a better understanding of feeding ecology in these groups.

METHODS

The specimens (see table 1) were scanned using the facilities of the SFR Bio-sciences (UMS3444/CNRS, US8/Inserm, ENS de Lyon, UCBL) AniRa-ImmOs. The herein presented specimens were scanned using a voxel size of 1.6 μm . The surfaces were extracted slice-by-slice using AVIZO 9.0 (Visualization Sciences Group) resulting in polygonal meshes composed of triangle. To reduce the noise related to segmentation artefacts, surfaces were smoothed under Meshlab software using the Taubin

smooth method (Taubin, 1995). Then, in order to avoid any bias induced by the disparate sizes of the triangular polygons composing meshes, triangle size was homogenized on the base of the mean size of mesh triangle using the Isotropic remeshing of Meshlab software. Finally, topographical indices were calculated and mapped using Doolkit package in R (Thiery et al. 2021).

Inv nr.	Taxon
UM CTB 082	<i>Bispathodus aculeatus</i>
UM CTB 083	<i>Bispathodus aculeatus</i>
UM CTB 086	<i>Bispathodus aculeatus</i>
UM CTB 088	<i>Bispathodus ultimus</i>
UM CTB 089	<i>Bispathodus aculeatus</i>
UM CTB 090	<i>Bispathodus costatus</i>
UM CTB 092	<i>Bispathodus ultimus</i>
UM CTB 093	<i>Bispathodus costatus</i>
UM CTB 094	<i>Bispathodus spinulicostatus</i>
UM CTB 096	<i>Bispathodus aculeatus</i>
UM CTB 098	<i>Bispathodus ultimus</i>
UM CTB 060	<i>Bispathodus costatus</i>
UM CTB 073	<i>Bispathodus spinulicostatus</i>
UM CTB 049	<i>Branmehla suprema</i>
UM CTB 100	<i>Branmehla inornata</i>
UM CTB 101	<i>Bispathodus stabilis</i>
UM CTB 102	<i>Branmehla suprema</i>
UM CTB 103	<i>Branmehla suprema</i>
UM CTB 104	<i>Branmehla suprema</i>
UM CTB 105	<i>Branmehla suprema</i>
UM CTB 106	<i>Branmehla suprema</i>
UM CTB 072	<i>Branmehla suprema</i>
UM CTB 107	<i>Branmehla suprema</i>
UM CTB 108	<i>Branmehla suprema</i>
UM CTB 109	<i>Branmehla suprema</i>
UM CTB 110	<i>Bispathodus stabilis</i>
UM CTB 112	<i>Palmatolepis gracilis</i>
UM CTB 061	<i>Palmatolepis gracilis</i>
UM CTB 115	<i>Palmatolepis gracilis</i>
UM CTB 116	<i>Palmatolepis gracilis</i>
UM CTB 117	<i>Palmatolepis gracilis</i>
UM CTB 062	<i>Palmatolepis gracilis</i>
UM CTB 118	<i>Palmatolepis gracilis</i>
UM CTB 119	<i>Palmatolepis gracilis</i>
UM CTB 120	<i>Palmatolepis gracilis</i>
UM CTB 075	<i>Polygnathus communis</i>
UM CTB 121	<i>Polygnathus communis</i>
UM CTB 122	<i>Polygnathus communis</i>
UM CTB 123	<i>Polygnathus communis</i>
UM CTB 125	<i>Polygnathus communis</i>
UM CTB 126	<i>Polygnathus communis</i>
UM CTB 128	<i>Polygnathus communis</i>
UM CTB 130	<i>Polygnathus communis</i>
UM CTB 131	<i>Polygnathus communis</i>
UM CTB 132	<i>Polygnathus communis</i>
UM CTB 133	<i>Polygnathus communis</i>
UM CTB 139	<i>Polygnathus symmetricus</i>

UM CTB 140	<i>Polygnathus symmetricus</i>
UM CTB 141	<i>Polygnathus symmetricus</i>
UM CTB 142	<i>Polygnathus symmetricus</i>

Table 1. List of P element models. Collection: University Montpellier, Institut des Sciences de l’Evolution.

ACKNOWLEDGEMENTS

The authors acknowledge the platform of microtomography of SFR Bio-sciences (UMS3444/CNRS, US8/ Inserm, ENS de Lyon, UCBL), Carlo Corradini for helping us in specimen determination and Felix Nesme for helping us sampling on the field. This study was performed through the ERJ project ICONE supported by LabEx CeMEB, an ANR “Investissements d’avenir” program (ANR-10-LABX-04-01). This is publication ISEM 2024-010.

BIBLIOGRAPHY

- Aldridge, R.J., 1987. Conodont palaeobiology: An historical review. In: Palaeobiology of Conodonts. Ellis Horwood, Chichester, pp. 11–34.
- Clark, D.L., 1983. Extinction of Conodonts. Journal of Paleontology 57 (4), 652–661
- Donoghue, P.C.J., Purnell, M.A., 1999. Mammal-like occlusion in conodonts. Paleobiology 25 (1), 58–74.
- Evans, A.R., Wilson, G.P., Fortelius, M., Jernvall, J., 2007. High-level similarity of dentitions in carnivorans and rodents. Nature 445 (7123), 78–81. <https://doi.org/10.1038/nature05433>
- Girard, C., Renaud, S., Serayet, A., 2004. Morphological variation of *Palmatolepis* Devonian conodonts: species versus genus. Comptes Rendus Palevol 3 (1), 404–415. <https://doi.org/10.1016/j.crpv.2003.09.008>
- Goudemand, N., Orchard, M.J., Urdy, S., Bucher, H., Tafforeau, P., 2011. Synchrotron-aided reconstruction of the conodont feeding apparatus and implications for the mouth of the first vertebrates. Proceedings of the National Academy of Sciences 108 (21), 8720–8724. <https://doi.org/10.1073/pnas.1101754108>
- Guenser, P., Souquet, L., Doledec, S., Mazza, M., Rigo, M., Goudemand, N., 2019. Deciphering the roles of environment and development in the evolution of a late Triassic assemblage of conodont elements. Paleobiology 45 (3), 1–18. <https://doi.org/10.1017/pab.2019.14>
- Guy, F., Gouvard, F., Boistel, R., Euriat, A., Lazzari, V., 2013. Prospective in (Primate) Dental analysis through tooth 3D topographical quantification. PLoS One 8 (6), e66142. <https://doi.org/10.1371/journal.pone.0066142>
- Hogancamp, N.J., Barrick, J.E., Strauss, R.E., 2016. Geometric morphometric analysis and taxonomic revision of the Gzhelian (late Pennsylvanian) conodont *Idiognathodus* simulator from North America. Acta Palaeontologica Polonica 61 (3), 477–502. <https://doi.org/10.4202/app.00198.2015>
- Jones, D., Purnell, M.A., Von Bitter, P.H., 2009. Morphological criteria for recognising homology in isolated skeletal elements:

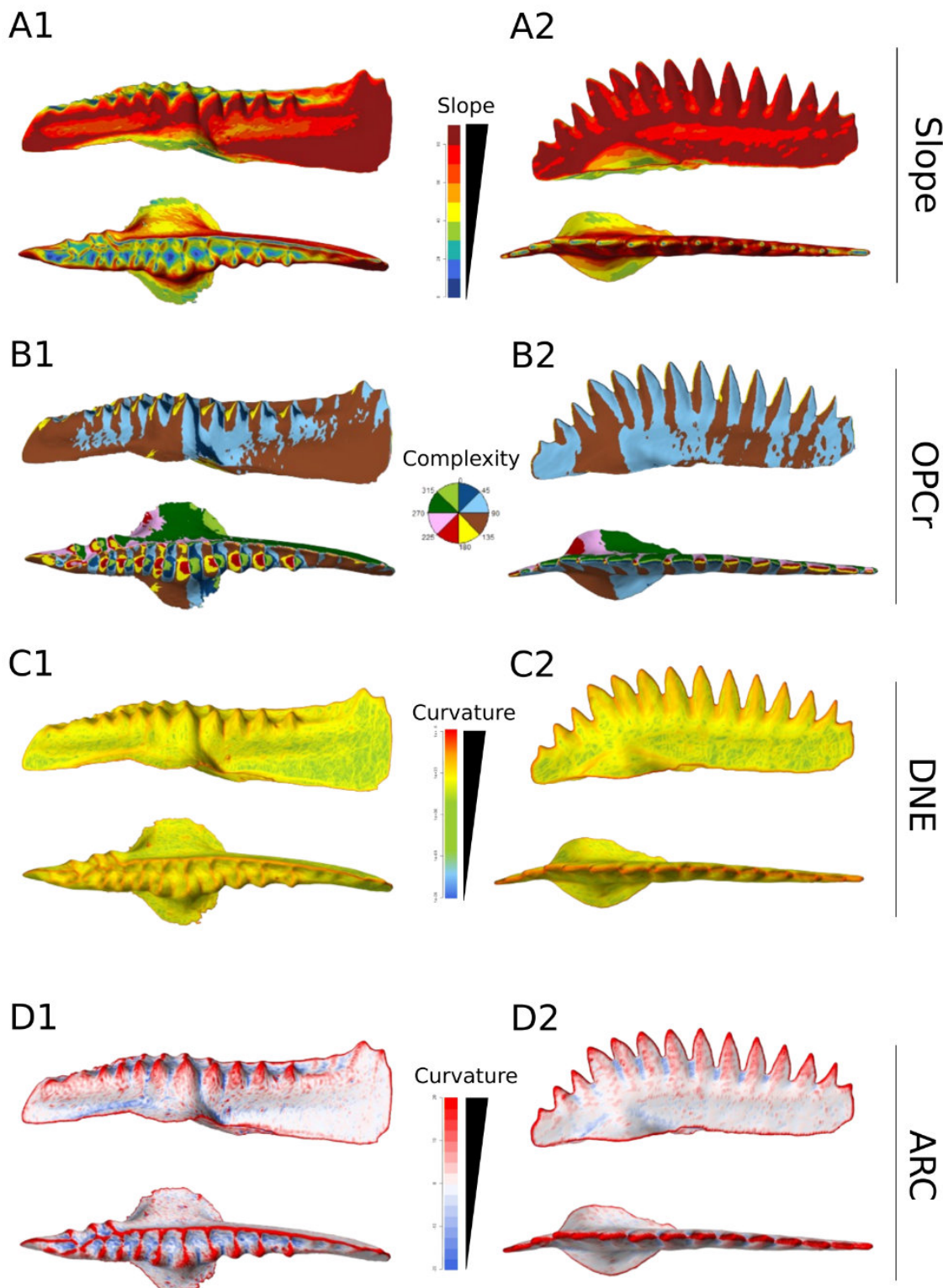


Figure 1. Mapping of topographic indices on P elements of two conodont taxa illustrating two different morphologies highlighting the differences between: 1- the wide platform *Bispathodus ultimus*, 2- the blade like *Branmehla suprema*. Indexes of complexity: A- Slope, B- OPCr. Indexes of curvature and sharpness: C- DNE, D- ARC

- comparison of traditional and morphometric approaches in conodonts. *Palaeontology* 52 (6), 1243–1256. <https://doi.org/10.1111/j.1475-4983.2009.00915.x>
- Li, P., Morse, P.E., Kay, R.F., 2020. Dental topographic change with macrowear and dietary inference in *Homunculus patagonicus*. *Journal of Human Evolution* 144 <https://doi.org/10.1016/j.jhevol.2020.102786>
- Martinez-Perez, C., Plasencia, P., Jones, D., Kolar-Jurkovsek, T., Sha, J., Botella, H., Donoghue, P.C., 2014a. There is no general model for occlusal kinematics in conodonts. *Lethaia* 47 (4), 547–555. <https://doi.org/10.1111/let.12080>
- Martinez-Perez, C., Rayfield, E.J., Purnell, M.A., Donoghue, P.C., Johanson, Z., 2014b. Finite element, occlusal, microwear and microstructural analyses indicate that conodont microstructure is adapted to dental function. *Palaeontology* 57 (5), 1059–1066. <https://doi.org/10.1111/pala.12102>
- Over, D.J., 1992. Conodonts and the Devonian-Carboniferous Boundary in the Upper Woodford Shale, Arbuckle Mountains, South-Central Oklahoma. *Journal of Paleontology*. 66 (2), 293–311. <https://doi.org/10.1017/S0022336000033801>
- Prufrock, K.A., Boyer, D.M., Silcox, M.T., 2016. The first major primate extinction: an evaluation of paleoecological dynamics of north American stem primates using a homology free measure of tooth shape. *American Journal of Biological Anthropology* 159, 683–697. <https://doi.org/10.1002/ajpa.22927>.
- Purnell, M.A., 1995. Microwear on conodont elements and macrophagy in the first vertebrates. *Nature* 374 (6525), 798–800. <https://doi.org/10.1038/374798a0>
- Purnell, M.A., Donoghue, P.C.J., 1997. Architecture and functional morphology of the skeletal apparatus of ozarkodinid conodonts. *Philosophical Transactions: Biological Sciences*. 352, 1545–1564. <https://doi.org/10.1098/rstb.1997.0141>
- Purnell, M.A., Donoghue, P.C., Aldridge, R.J., 2000. Orientation and anatomical notation in conodonts. *Journal of Paleontology*. 74 (1), 113–122. [https://doi.org/10.1666/0022-3360\(2000\)074<113:OAANIC>2.0.CO;2](https://doi.org/10.1666/0022-3360(2000)074<113:OAANIC>2.0.CO;2)
- Suttner, T.J., Kido, E., Briguglio, A., 2017. A new icriodontid conodont cluster with specific mesowear supports an alternative apparatus motion model for Icriodontidae. *Journal of Systematic Palaeontology* <https://doi.org/10.1080/14772019.2017.1354090>
- Sweet, W.C., 1981. Macromorphology of elements and apparatuses. In: Clark, D.L., Sweet, W.C., Bergstrom, S.M., Klapper, G., Austin, R.L., Rhodes, F.H.T., Müller, K.J., Ziegler, W., Lindstrom, M., Miller, J.F., Harris, A.G. (Eds.), *Treatise on Invertebrate Paleontology Part W Miscellanea Supplement 2 Conodonts, 5-20*. Geological Society of America. Boulder, Colorado, and University of Kansas Press, Lawrence, Kansas.
- Sweet, W.C., 1988. The Conodont Morphology, Taxonomy, Paleoecology and Evolutionary history of a Long-Extinct Animal Phylum. In: Oxford Monographs on Geology and Geophysics No. 10. Oxford University Press, Oxford., p. 212
- Taubin, G., 1995. Curve and surface smoothing without shrinkage. In: *Proceedings of IEEE International Conference on Computer Vision*.
- Thiery, G., Guy, F., Lazzari, V., 2021. Doolkit: Exploration of Dental Surface Topography. R Package. <https://cran.r-project.org/web/packages/doolkit/index.html>
- Ungar, Peter and Williamson, Malcolm 2000. Exploring the Effects of Toothwear on Functional Morphology: A Preliminary Study Using Dental Topographic Analysis. *Palaeontologia Electronica*, vol. 3, issue 1, art. 1: 18pp. https://palaeo-electronica.org/2000_1/gorilla/main.htm
- Winchester, J.M., 2016. MorphoTester: an Open Source Application for Morphological Topographic Analysis. *PLoS One* 11 (2). <https://doi.org/10.1371/journal.pone.0147649>